

Bridging Organometallics and Quantum Chemical Topology: Understanding Electronic Relocalisation During Palladium-Catalyzed Reductive Elimination

Benoit de Courcy,^[a] Etienne Derat,^{*,[b]} and Jean-Philip Piquemal^{*,[a]†}

This article proposes to bridge two fields, namely organometallics and quantum chemical topology. To do so, Palladium-catalyzed reductive elimination is studied. Such reaction is a classical elementary step in organometallic chemistry, where the directionality of electrons delocalization is not well understood. New computational evidences highlighting the accepted mechanism are proposed following a strategy coupling quantum theory of atoms in molecules and electron localization function topological analyses and enabling an extended quantification of donated/back-donated electrons fluxes along reaction paths going beyond the usual Dewar–Chatt–Duncanson model. Indeed, if the ligands coordination mode (phosphine, carbene) is commonly described as dative,

it appears that ligands lone pairs stay centered on ligands as electrons are shared between metal and ligand with strong delocalization toward the latter. Overall, through strong trans effects coming from the carbon involved in the reductive elimination, palladium delocalizes its valence electrons not only toward phosphines but interestingly also toward the carbene. As back-donation increases during reductive elimination, one of the reaction key components is the palladium ligands ability to accept electrons. The rationalization of such electronic phenomena gives new directions for the design of palladium-catalyzed systems. © 2015 Wiley Periodicals, Inc.

DOI: 10.1002/jcc.23911

Introduction

One of the main purposes of modern organic chemistry is to build carbon–carbon bond in an efficient manner, generally by using a catalyst used in substoichiometric amount and inducing good selectivities. In this framework, homogenous palladium catalysis has proven in the last decades to be of particular interest. Usually, palladium-based catalyst is used with an organic halide, and an organometallic or main-group reagent as the other nucleophilic coupling partner,^[1] although coupling based on C–H activation has recently emerged as an interesting route.^[2] Stille (with organotin as the nucleophile),^[3] Kumada (organomagnesium Negishi (organozinc)),^[4,5] Suzuki–Miyaura (organoboron),^[6] Hiyama–Denmark (organosilicon) couplings^[7] are well established. One can also notice that the coupling of two different organic halides is known, for example in the Catellani reaction.^[8] During palladium-catalyzed reactions, a classification of the various elementary steps can help to rationalize the mechanism: oxidative addition, transmetalation, β -hydride elimination, reductive elimination and so on.^[9] But what remains as the common point between all the previously cited reactions is the fact that they shared an elementary act during which the key CC bond is formed: the one called reductive elimination.

But despite its importance in organometallic chemistry, the reductive elimination has not been so thoroughly studied from a theoretical point of view.^[10] Indeed, from a computational aspect, there are a huge number of studies calculating energetic barriers related to this process and examining the various possibilities in term of (regio/diastereo/enantio) selectivity. But rationalization of the process is much scarcer. There

is a few theoretical papers showing that π -accepting ligands accelerate the rate of the reductive elimination.^[11] However, they do not propose a detailed view of the electrons rearrangements. The goal of this study is to examine the fate of valence electrons involved during the process of reductive elimination catalyzed by various Pd(II) complexes, namely in conjunction with different phosphines (see Scheme 1, system A) and carbene (see Scheme 1, system B). By covering various ligands, one can expect that through this theoretical study will emerge the electronic guideline behind the reductive elimination. As shown by recent experimental studies, the reductive elimination process is a key component^[12] and still a debated subject at the forefront of modern organometallic catalysis.

Recently, Lei et al. have shown in an elegant mechanistic study on C(sp)–C(sp) palladium-catalyzed coupling that the rate of the reductive elimination is strongly dependent on the nature of the phosphine.^[13] When using a good π -acceptor phosphine, they demonstrated through *in situ* infrared analyses that the rate of reductive elimination is significantly accelerated and favored hetero-coupling rather than

[a] B. de Courcy, J.-P. Piquemal

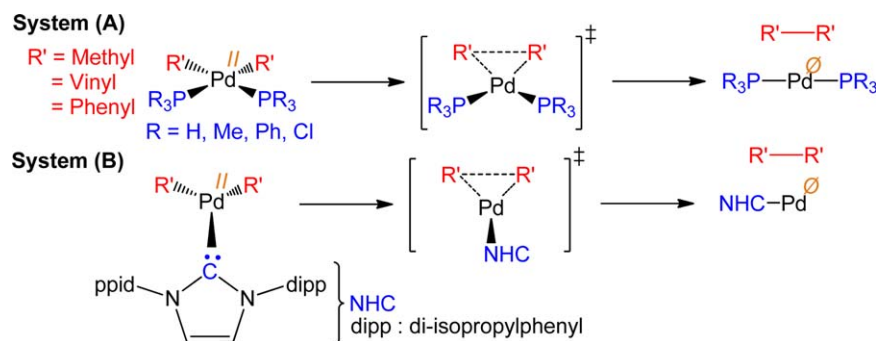
Sorbonne Universités, UPMC Univ Paris 06, UMR 7616, Laboratoire de Chimie Théorique, Case courrier 137, 4 place Jussieu, 75005 Paris, France
E-mail: jpp@lct.jussieu.fr

[b] E. Derat

Sorbonne Universités, UPMC Univ Paris 06, UMR 720, Institut Parisien de Chimie Moléculaire, Case courrier 229, 4 place Jussieu, 75005 Paris, France
E-mail: etienne.derat@upmc.fr

*Indeed as selectivity is governed by subtle effects, minor variation on the phosphine can have a major impact on observed experimental product.

© 2015 Wiley Periodicals, Inc.



Scheme 1. Description of the reductive elimination reaction within the proposed systems. [Color figure can be viewed in the online issue, which is available at wileyonlinelibrary.com.]

homo-coupling. The same trends have been observed with carbene ligands but not with Pd. For example, in 2010, Fürstner and Thiel showed^[14] that the capacity of a N-heterocyclic carbene (NHC) can affect the outcome of a gold-catalyzed reaction. A strong π -acceptor carbene was able to selectively produce [2 + 2] cycloaddition product, whereas more classical NHC were inducing [3 + 2] cycloaddition. Previously, Hartwig has reviewed the trends regarding the kinetics of the reductive elimination.^[15] The main trend is that organometallic complexes with electron-donating ligands are predicted to undergo reductive elimination slower than complexes with less electron-donating ligands. But Hartwig also noticed in its concluding remarks that plenty of counterexamples can be found in literature^[16] and eventually asserted that « a theoretical explanation for these electronic effects awaits additional modern computational work ».

In transition metal complexes, the model of Dewar–Chatt–Duncanson^[17] (DCD) proposes to divide interactions into a donation contribution associated to σ bonds and a back-donation related to π bonds. Such model has been shown to be incredibly useful to chemists over the years and benefited from the use of quantum mechanical methods.^[18–20] Today, it remains a conceptual tool to rationalize the bonding in metal–ligand complexes. Various quantum methods ranging from energy decomposition (EDA) analyses^[18–21] to Valence Bond^[22] have been proposed to successfully illustrate these bonding patterns. However, for complex organometallic systems the mandatory attribution of charge/spin states to well-defined molecular fragments and/or the strong covalency forbids the use of EDA approaches, whereas the computational cost of full Valence Bond computations is yet out of reach. We propose to revisit the DCD model of bonding in metal–ligands complexes by means of quantum chemical topological approaches that rely only on the post-processing of electronic densities extracted from popular quantum chemistry packages along any reaction path. Therefore, in this contribution, the discussed classical elementary organometallic reaction (i.e., the reductive elimination) will be analyzed thanks to state of the art computational interpretative techniques such as the electron localization function topological analysis (ELF)^[23] and its coupling^[24] to the QTAIM (quantum theory of atoms in molecules).^[25] Indeed, ELF enables a chemically intuitive partition of molecular regions involving strong electron pairing such as atoms,

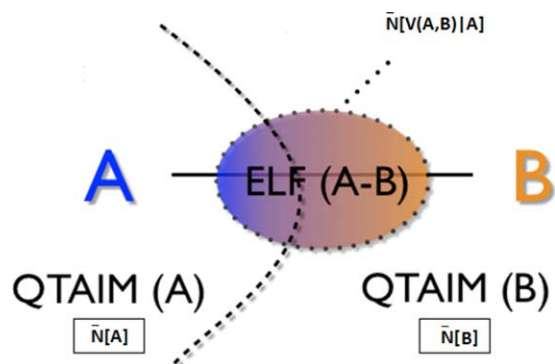
bonds, and lone pairs, whereas QTAIM offers an atom-centered vision of the electronic density. The coupling of the two methods offers us a way to discuss the sharing of bonding electrons within such complex organometallic systems (see Scheme 2 and following method section). Previous work has been done with QTAIM on palladium-catalyzed reductive elimination,^[26] but the analysis mainly focuses on the energetic trends and not on the intimate electronic rearrangement occurring during the process. Moreover, following recent works,^[27] complete reaction paths on various chemically relevant systems and including the transition state will be under the scrutiny of the QTAIM/ELF methodology.

Methods

Quantum chemical topology

In this section, we describe the strategy used to quantify bonding in metal–ligands complexes by means of quantum chemical topological approaches that rely only on the post-processing of electronic densities extracted from popular quantum chemistry packages along any reaction path.

To do so, following recent studies, showing it was possible to couple known topological methods to extend the analysis capabilities,^[24] we propose to use computational strategy to unravel



Scheme 2. QTAIM/ELF topological partition ($n e^-$ designates the number of electrons). For a given atom A, the QTAIM contribution for the atom A to the ELF bond $V(A,B)$ can be extracted, being noted $\bar{N}[V(A,B)|A]$ (following notations of Ref. [24a]) To evaluate donated and back-donated electrons (see text). [Color figure can be viewed in the online issue, which is available at wileyonlinelibrary.com.]

donation (ligand→metal) and back-donation (metal→ligand) electrons transfers based on the coupling of QTAIM and ELF electronic density partitions. Such an approach can be seen as a more general view of bonding than the traditional DCD model as described initially by Silvi and coworkers^[24] e,f] The two topological analyses approaches are used here synergistically. In such methods, the molecular space is partitioned using the theory of gradient dynamical systems leading to a set of molecular volumes or domains localized around maxima of the vector field of a scalar function. Therefore, using the same density grid extracted from a reaction path, we perform two types of partition of the molecular space. First, the electron density is divided into Bader's atom following the QTAIM strategy that uses the electronic density itself as local function through a topological analysis of its Laplacian. Second, on the electronic density we compute the ELF that will be also used as a local function to perform a topological analysis of the ELF gradient field. Indeed, ELF can be seen as a signature of the electronic pair distribution and is defined to vary between 0 and 1 making it easy to compute and interpret. One advantage of ELF is that it is not restricted to atoms but proposes a chemically intuitive description of the electronic density organization enabling to separate core electrons (denoted as C) that are localized on the nuclei from valence electrons (denoted as V) that expand beyond the nuclei positions, such as lone pairs or that are shared between atoms forming bonds and π systems. In both cases, it is possible to integrate the density within QTAIM or ELF domains to recover the local number of electrons (populations noted \bar{N}). The central idea here is simple and is depicted on Scheme 2. If one analyzed the assignments of each density grid points between a metal atom and its ligands, there will be grid points belonging to a given QTAIM atom A that also belongs to a bond associated to an ELF domain that is shared between the two atoms A and B. In this picture, computing the number of donated (ligand→metal) and back-donated (metal→ligand) electrons is straightforward as it involves only the populations of the QTAIM interacting atoms, namely the metal (M) and the heavy atom (X) of the ligand involved in the covalent bond (denoted M–X) whose population can be unraveled using ELF. $\bar{N}[V(M,X)|M]$ and $\bar{N}[V(M,X)|X]$ are then the respective contributions of the Metal and of the ligand to the bond (following following Ref. [24e,f] (see Scheme 2).

Constrained space orbital variation computations

Such analysis is helpful as it is known that there is little relation between the calculated density around an atom and the charge that is deduced from formal oxidation number counting^[24] with evident application to organometallics.

To ensure the validity of such coupled partitioning that is only based on the integration of a single electronic density grid, we propose to compare our approach to the constrained space orbital variation energy (CSOV) decomposition analysis, a molecular orbital scheme allowing discussing the energetics of the bondings within a metal–ligand.^[19,21,28]

In the CSOV scheme, the total binding energy (ΔE) between the cation and the ligand is decomposed in several physical terms.

$$\Delta E_{\text{int}} = E_c + E_{\text{exch-rep}} + E_{\text{polA}} + E_{\text{polB}} + E_{\text{CT(A} \rightarrow \text{B)}} + E_{\text{CT(B} \rightarrow \text{A)}} + \delta E$$

The first two terms result from the frozen molecular orbitals of the isolated fragments and represent the coulomb electrostatic interaction (E_c) and the Pauli/exchange-repulsion ($E_{\text{exch-rep}}$) contributions. Then, as the orbitals of the two fragments are progressively relaxed through the successive definition of variational spaces, the polarization energy (E_{pol}), that is, the distortion of the orbital of a fragment in the field generated by the “frozen” fragment is computed; followed by the charge transfer energy (E_{ct}), that is, the contribution of electron transfer from occupied orbitals of one fragment to the vacant orbitals of the other fragment. The last term (δE) accounts for some higher-order many-body terms from different physical origins that are not detailed in the standard RVS decomposition; they are expected to be negligible with respect to ΔE . The possibility of extracting charge transfer in both directions, that is, $E_{\text{CT(A} \rightarrow \text{B)}}$ and $E_{\text{CT(B} \rightarrow \text{A)}}$, is explicitly related to the definition of ligand (L)–metal (M) donation ($E_{\text{CT(L} \rightarrow \text{M)}}$) and back-donation ($E_{\text{CT(M} \rightarrow \text{L)}}$) in the DCD model. It is important to point out that in the DCD model, back-donation only concerns the electron donation from the metal to the empty orbitals of π symmetry. In CSOV and within the QTAIM/ELF topological approach, no symmetry constraints are imposed. Therefore, the Metal to Ligands transfers concern donation to orbitals of all symmetries (σ and π), even though the tradition backdonation of π symmetry is an important component.

Single point CSOV computations were performed on optimized geometries at the B3LYP/Def2-TZVP level of theory. Harmonic frequencies computations were then performed to ensure real minima. For consistency, the EDA was realized using the same level of theory (B3LYP/Def2-TZVP). Before it, a single point calculation on fragments (i.e., Pd(0) and Ligand) was performed separately to obtain the corresponding molecular orbitals, then used in the CSOV calculation to ensure full convergence. As pointed out by Pacchioni and Bagus,^[21] the basis set superposition error (BSSE) is expected to be very small due to the use of a triple zeta basis set. Therefore, no BSSE correction posttreatment was performed here.

The important point is the possibility of extracting “directional” charge transfer contributions, that is, $E_{\text{CT(A} \rightarrow \text{B)}}$ and $E_{\text{CT(B} \rightarrow \text{A)}}$, that are explicitly related to the definition of ligand (L)–metal (M) donation ($E_{\text{CT(L} \rightarrow \text{M)}}$) and back-donation ($E_{\text{CT(M} \rightarrow \text{L)}}$) in the DCD model. Although usually restricted to Hartree–Fock, the CSOV approach can include correlation through density functional theory (DFT)^[26] (and some specific applications to multi-configurational self-consistent field (MCSCF)^[27]). Various typical Pd(0)–L complexes ($L = \text{NH}_3, \text{PH}_3, \text{CH}_2, \text{PF}_3, \text{PMe}_3, \text{POMe}_3$) from the literature^[19,20] and encompassing atoms encountered in this study are detailed as test-cases in Table 1. Trends are found in very good agreement between the results of the QTAIM/ELF electron fluxes and CSOV energies at the DFT (B3LYP) level. Indeed, ligands range from NH_3 that encompasses an almost null back-donation CSOV contribution associated to a very small Pd contribution to the bond, to the CH_2 carbene that exhibits strong back-donation energy along with a metal that contributes strongly to the formation of the more

Table 1. CSOV energy decomposition analysis (charge transfer contributions only) and the corresponding electron populations of the palladium-ligands bonds for six Pd(0) complexes.

CSOV (B3LYP) (kcal/mol)	NH ₃	PMe ₃	PH ₃	P(OMe) ₃	PF ₃	CH ₂
L→Pd(0) donation	-15.0	-30.6	-24.7	-29.2	-25.7	-24.6
Pd(0)→L back-donation	-4.5	-20.8	-22.9	-23.8	-33.0	-27.9
QTAIM/ELF (B3LYP) (number of e ⁻)	NH ₃	PMe ₃	PH ₃	P(OMe) ₃	PF ₃	CH ₂
Contribution of X to the V(Pd(0),X) bond	1.77	1.77	1.78	1.98	2.21	1.82
Contribution of Pd(0) to the V(Pd(0),X) bond	0.11	0.49	0.50	0.53	0.60	0.64
Total V(Pd(0),X) bond	1.88	2.26	2.28	2.51	2.81	2.46
X =	N	P	P	P	P	C

covalent bond. Although not providing a direct energetical view, the QTAIM/ELF approach is based only on electronic density and potentially applicable to any type of correlated methods. Coupling QTAIM and ELF is consistent as both approaches use the same density grid and topological electron population integration techniques. As the approach deals with electron population, such strategy should enable use a discussion beyond the strict idea of formal charges. Therefore, such simple coupling strategy enables to discuss the DCD model by unraveling and quantifying directional electron fluxes and is applicable to the study of bondings in large systems of interest in organometallic chemistry.

Computational details

Except for CSOV computations (see section above), all complexes for system A (except for PPh₃) have been structurally optimized at the M06^[28] level of theory with the Def2-TZVP basis set^[29] that combines an all electron TZVP basis set for H, C, Cl, and P atoms with the small core (28 electrons) Def2 pseudo-potential for palladium. Some complexes have been reoptimized in the presence of a solvent tetrahydrofuran (THF) using the polarizable continuum model to ensure that no significant effect of the solvent is observed on the complexes' geometry. Single point calculations have been performed on selected small size complexes using the all electron aug-cc-pVTZ-DK basis set^[30] on all atoms to verify the appropriateness of the use of the Def2 pseudo-potential for palladium. Compared with the all-electron basis set, the use of the pseudo-potential reveals only a very slight underestimation of the back-donation trends described in the text, which makes the pseudo-potential approach suitable to describe such systems. Due to their larger sizes, system A (PPh₃) and system B were geometrically optimized at the M06/Def2-SVP level of theory using a smaller double zeta basis set, then underwent a single point calculation using the same Def2-TZVP basis set for consistency. Tests have been done by directly optimizing a large complex with the TZVP basis set: only very minor changes were observed compare to the SVP geometry. In all cases, analytical frequency computations were performed to ensure real minima. All calculations have been performed using the Gaussian 09, Revision A.02 package^[31] except for the CSOVs that were performed using a modified version of HONDO 95.3.^[32] For the CSOV discussion, all CSOV and ELF/

AIM computations were performed at the B3LYP/Def2-TZVP level. ELF and QTAIM computations were performed using the TopMod package^[33] using steps of 0.1 a.u. between grid points. The coupled QTAIM/ELF analysis is therefore, performed automatically, the program providing atomic QTAIM contributions to any ELF bond domain.

Results and Discussion

Phosphine complexes

The detailed reactions energetic profiles (Gibbs free energies) can be found for all the studied complexes and reaction paths in Supporting Information S1. The detailed QTAIM/ELF partition results can be found for all the studied complexes and reaction paths in Supporting Information S2.

To exemplify the electronic distribution within a palladium complex, the reagent adduct of system A with triphenylphosphine ligands will serve as a test case to introduce the QTAIM/ELF partition. The pictorial analysis for this complex is given in Figure 1.

The ELF function is able to differentiate between the core, valence, and lone pairs electrons. Thus on Figure 1, the spherical shapes around the nuclei correspond to the core electrons of the respective atoms. The four domains localized around the palladium core are attributed to the d electrons belonging to the metallic center and not shared covalently with the surrounding partners. These electrons are usually named subvalence. What is interesting to notice is the fact that these subvalence^[34] domains are mutually avoiding the four bonding axis, which is a proof that the electrons responsible for these domains are not involved in the corresponding bondings. Between the palladium core and the carbons of the coupling phenyls, two domains are found: they represent the electrons associated to the covalent bonds. One can notice that these domains are rather contracted and polarized toward the carbon cores. The electronic populations of these two domains are found to be about 1.78 and 1.82 electrons, which is due to the slight asymmetrical nature of the complex. It is worth to notice that around 0.2 electrons are missing; this is challenging the classical point of view of a anionic carbon bonded to palladium^[35] The QTAIM/ELF partition reveals that, respectively, 0.22 and 0.23 electrons are provided by the palladium while the other parts are obviously coming from the carbons (1.56

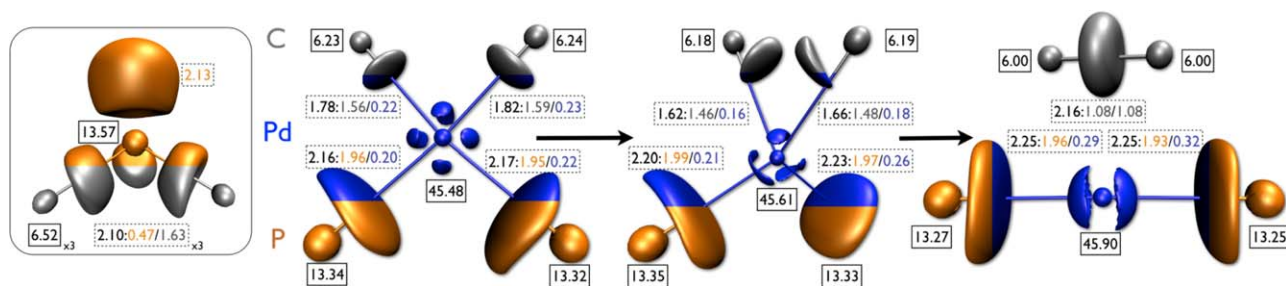


Figure 1. ELF representation for the three states (reagent, TS, product) involved in the reductive elimination process (System A, $R = \text{Ph}$, $R' = \text{Ph}$). For clarity purpose, only the coordinating atoms and palladium are depicted. Domains are colored according to the atomic contributions (phosphorus in orange, palladium in dark blue, and carbon in grey). Numbers enclosed in boxes correspond to QTAIM population (in term of number of electrons) while dotted boxes give the ELF bond partitioning (total population involved in the bond and contribution from each partner, again in number of electrons). The picture only displays a few atoms, that is, the Pd coordination, where the back-donation takes place. However, the ligand exhibits variations of populations between R, TS, and P states as electrons relocalized themselves on other parts of the systems. Of course, the total number of electrons within the whole system remains constant whereas the proposed zoom does not, by definition, requires to have a constant population.

and 1.59 e-). The two remaining domains are the ones localized between the palladium and the phosphines (PPh₃). They are broader than the Pd-C domains, reflecting the dative nature of this bonding (65.8 a.u.^[3] vs. 33.3 a.u.^[3] for Pd-P and Pd-C domains volumes, respectively). But what is amazing is that the electron partition gives 2.17 and 2.16 electrons in each of these domains. Neighbours, thus, enrich the palladium-phosphorus bond. Again the QTAIM/ELF analysis allows understanding from where the electrons are coming from: namely 0.20 and 0.22 electrons are provided by the metallic center and 1.96 and 1.95 electrons are given by the phosphines. The current system is typically described as a Pd(II) complex, thus, bearing 44 electrons on the metal. The QTAIM/ELF calculations deliver a rather different value as 45.48 electrons were found. Thus, from the electronic structure partitioning is emerging a covalent type bonding rather than an ionic system. But the most stunning feature is the strong back-donation found in the palladium-phosphine bonds. This assertion is supported by the fact that the QTAIM/ELF partitioning specifies a value superior to two electrons for these bonds. The fact that the carbon-palladium bonds are depleted (around 1.8 e-) indicates that a trans effect is at work: nucleophilic carbons (6.23e- according to QTAIM) donate electrons, which are transferred throughout the palladium to the phosphorus ligands.^[36]

The same situation is observed in the corresponding reductive elimination transition state (Fig. 1B). As expected during this reduction process, the QTAIM analysis shows an increase of the electronic population on the palladium center (from 45.48 e- to 45.61 e-). This reduction is due to an electronic transfer from the reacting phenyl carbons, which is not a surprise. But what is striking is the stability of the phosphines' electronic structure, and the relative weight of the two palladium-phosphorus shared domains: 2.16e- in the reagent and 2.20 e- in the transition state. Thus, the same strong back-donation remains. Most probably, the electrons brought back from the nucleophilic carbons during the reductive elimination have been relocalized into the palladium-phosphorus bonds.

This analysis is confirmed by the QTAIM/ELF partitioning observed in the product: the total population on palladium is

now close to 46 electrons (exactly 45.90 e-) and the number of electrons localized into the palladium-phosphorus domains has now increased to 2.36 and 2.39 electrons. 0.33 and 0.37 e- are provided by the palladium center, while the phosphorus remain unchanged with 2.03 and 2.02 e-. The back-donation increases stepwise during the reductive elimination and is therefore, one of the driving-force of the process. It can be highlighted that the core subvalence of the metal is progressively reoriented along the bond axis (dark blue lobes on the palladium in Fig. 1) while the reductive elimination proceeds. This may explain why the phosphines stay coordinated to the reduced palladium despite its enrichment. The other driving force is obviously the formation of the strong C—C bond, which is confirmed by the QTAIM/ELF analysis of the C—C bond. Each carbon involved provides 1.08 electrons to form the covalent bond and its respective population is now exactly six electrons due to the symmetric nature of the created compound.

Carbene complexes

To probe our first conclusions on the previously exposed system, various systems were investigated. Namely, some variations on the phosphines, replacements of the phosphines by a carbene were also considered for ascertaining the transferability of the mechanism. The corresponding data can be found in Table 2. To respect the consistency, the phenyl groups of the phosphine were replaced by methyl, hydrogen, and chloride. While in the reagent and with PPh₃, 0.21 electrons are involved in the back-donation from the palladium to the phosphine (Table 2, third column), it was found that this value reaches 0.28 electrons with PMe₃, 0.23 electrons with PH₃ and 0.21 electrons with PCl₃. Thus, this phenomenon is much conserved across the phosphine family, the main effect being attributed to the interaction of palladium with the phosphorus nucleus and only minor variations are due to the substituent effects.* This trend is found similar in the transition state and in the product. Similarly, the lone pair of phosphorus is found quasi-identical across the phosphine family (Table 2, fourth column) except when substituted by chloride where ligands

Table 2. Atomic contributions to the palladium-phenyl and palladium-ligand bonds while varying palladium's ligands.

Phenyl—Phenyl	W_C in Pd-C			W_{Pd} in Pd-C			W_{Pd} in Pd-L			W_L in Pd-L			Energetic Levels (in kcal/mol)	
	R	TS	P	R	TS	P	R	TS	P	R	TS	P	Reagents →TS	Reagents → Product
System A/PPh ₃	1.57	1.46	1.08	0.22	0.17	N.A.	0.21	0.23	0.35	1.94	1.97	2.02	6.4	−37.0
System A/PMe ₃	1.57	1.43	1.10	0.28	0.20	N.A.	0.28	0.30	0.29	1.87	1.95	1.99	10.3	−30.3
System A/PH ₃	1.50	1.37	1.10	0.29	0.21	N.A.	0.23	0.23	0.27	1.87	1.93	1.96	5.5	−37.3
System A/PCl ₃	1.38	1.31	1.11	0.28	0.23	N.A.	0.21	0.23	0.32	2.11	2.14	2.25	1.3	−44.6
System B	1.54	1.42	1.10	0.23	0.19	0.13	0.18	0.18	0.23	2.36	2.36	2.36	2.2	−36.3

Legend: W_C stands for weight of the carbon within the Pd-C bond expressed in number of electrons. The next two columns give the weight of palladium within the Pd-C and the Pd-Ligand bonds respectively. W_L is the weight of the palladium ligand into the Pd-L bond: phosphorus included into various phosphines in System A, the carbene part of the NHC in System B. The two last columns give the energetical values (Gibbs free energies, in kcal/mol) of R, TS, P for all reaction paths.

populations are enhanced due to the hyperconjugative nature of the chloride lone pairs. Let's now focus on the palladium-carbon bond. As explained before, the weight of the palladium contribution decreases during the reductive elimination and a similar trend is observed with all the phosphines (Table 2, second column). Again, with all the phosphines, palladium electrons involved in the bonding with carbon are progressively transferred to the palladium-phosphorus bond, thus, increasing the back-donation along the reaction path. For system B, the same tendency emerges from the computational values as strong back-donation is observed. Therefore, the capacity of the ligands (phosphine or carbene) to accept electrons is an intrinsic phenomenon that overcomes the formal oxidation state of the metal. To complete our discussion, one can look at the behavior of Pd(0) (product) versus Pd(II) (reagent). It is exemplified by the trends observed for PMe₃, where the ligand is less electronically active than PPh₃. In that case, the ligand allows a weaker delocalization of the Pd electrons within itself

and therefore, the effect of the formal oxidation of Pd can be directly observed when going from Reagents to Products. We can see on Table 2 that the back-donation is constant along the reaction path which confirms that Pd(0) and Pd(II) are equally donor (see Table 2, line 1 and 2, column 3). For other ligands, the discussed molecules are all able to attract more significantly some of the Pd electrons (up to the electro attractive—Cl ligand). In that case, at the opposite of PMe₃, these ligands are electronically more active and therefore perturb the pure effect due to the change of the formal state of the metal. It is fully consistent with the experimental results as in fact, PMe₃ is known to be a less favorable ligand for the process. This is illustrated by the value of the barrier (see Table 2, columns 5 and 6 for the energetical values of R, TS, P for all reaction paths).

Regarding the carbene case (system B), and as shown in Figure 2, the QTAIM/ELF partitioning is very informative. In the reagent, a larger domain was found between palladium and

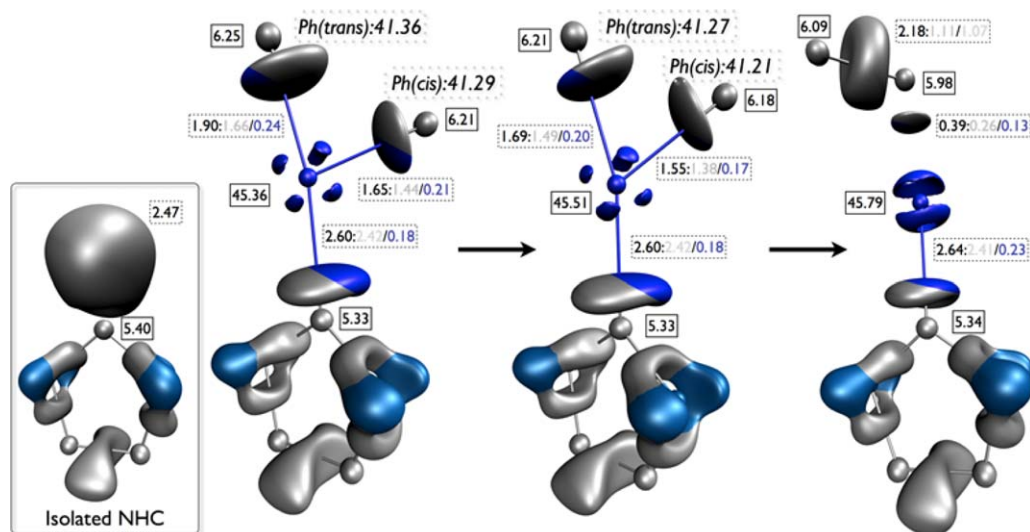


Figure 2. ELF representation of the three intermediates (reagent, TS, product) involved in the reductive elimination process (system B, NHC, $R' = \text{Ph}$). On the left side, in insert, ELF representation of the isolated carbene. For clarity purpose, only the coordinating atoms and palladium are depicted. Domains are colored according to the atomic contributions (palladium in dark blue, nitrogen in iceblue, and carbon in grey). Numbers enclosed in boxes correspond to QTAIM population, while dotted boxes give the ELF bond partitioning and are all expressed in number of electrons. Detailed ELF populations can be found for trans and cis phenyls in Supporting Information S4. [Color figure can be viewed in the online issue, which is available at wileyonlinelibrary.com.]

Table 3. Atomic contributions to the palladium-reactant and palladium-ligand bonds while varying the reactants.

	W_C in Pd-C			W_{Pd} in Pd-C			W_{Pd} in Pd-L			W_L in Pd-L		
System A												
PPh3	R	TS	P	R	TS	P	R	TS	P	R	TS	P
Phenyl—Phenyl	1.57	1.46	1.08	0.22	0.17	N.A.	0.21	0.23	0.35	1.94	1.97	2.02
Vinyl—Vinyl	1.43	1.34	1.09	0.27	0.24	0.19	0.21	0.23	0.28	1.96	1.97	1.98
Me—Me	1.11	0.84	0.91	0.26	0.14	N.A.	0.21	0.27	0.32	1.96	2.02	2.02
System B	R	TS	P	R	TS	P	R	TS	P	R	TS	P
Phenyl—Phenyl	1.54	1.42	1.10	0.23	0.19	0.13	0.18	0.18	0.23	2.36	2.36	2.36
Vinyl—Vinyl	1.41	1.31	1.09	0.26	0.22	0.21	0.18	0.18	0.20	2.34	2.36	2.36
Me—Me	1.02	0.86	0.92	0.26	0.12	N.A.	0.16	0.19	0.27	2.32	2.35	2.32

Legend: W_C stands for weight of the carbon within the Pd-C bond expressed in number of electrons. The next two columns give the weight of palladium within the Pd-C and the Pd-Ligand bonds respectively. W_L is the weight of the palladium ligand: phosphorus included into PPh3 for System A, the carbene part of the NHC in System B.

carbene than for phosphine. Obviously, it can be attributed to a strong interaction of the nitrogen lone pair to the π system of the NHC. To ascertain this, calculations on the NHC without palladium were performed; the coordination of the metal enriches the NHC by around 0.2 electrons (see Supporting Information, S3). Regarding the bonding of the phenyl groups, it is worth to notice that there is an obvious dissymmetric pattern due to the mono-coordination of the carbene. The phenyl group in trans to the carbene donates more electrons (1.66 e⁻) and thus, the domain is electron richer compare to the cis phenyl group. This latter is involved by only 1.44 electrons. In both cases the palladium has only minor contribution to the bonding (trans: 0.24 e⁻, cis: 0.21 e⁻). When the carbene is coordinated to the palladium, the carbene lone pair domain increases by 0.13 electrons (2.60 electrons are found in the carbene-palladium bond domain, while the carbene lone pair domain contains 2.47 electrons). As the richer (trans) carbon-palladium bond can donate by trans effect in this bonding, the electrons in excess on the carbene originate from the trans phenyl group, the global charge of the cis phenyl group being 0.15 electrons more than the trans one. Once again, the donation from the alkyl/vinyl/aryl groups is transmitted by back-donation to the accepting electrons ligands. The same phenomenon, as previously observed in the phosphine case, occurs within the transition state. Finally, the QTAIM/ELF partitioning tells us that the palladium is effectively reduced, moving from 45.36 electrons in the starting reagent to 45.79 electrons in the final product. Nevertheless, in the carbene case, the biphenyl remains coordinated to the palladium through a weak η^2 interaction. One can notice that there is a slight increase of the back-donation during the reaction process (0.18 e⁻ in the reagent to 0.23 e⁻ in the product).

While in Table 2, various palladium ligands were considered, in Table 3 palladium ligands were kept unchanged, only the substituents (phenyl, vinyl, and methyl) were modified to check the electronic reorganization emanating from them. Both system A (with triphenyl phosphine) and system B (carbene) were studied. Electronic populations shown here are remarkably conserved among the last three columns, demonstrating that there is almost no effect of the reactants on the palladium's back-donation and no effect on the palladium's ligands either. One can notice that, in both systems for the vinyl group and in system A for the phenyl group, the palladium still donates some electrons as the product remains coordinated to the catalyst, as seen in Figure 2. The sole

real difference appears in the first column, where the populations borne by the coordinating carbons decreases according to the richness in electron of the entire moiety considered; the phenyl the richer, the methyl the poorer. Along the reaction path however, the same trend is observed, that is a decrease of the carbon's population to reach approximately the same amount of bound electrons (0.91 to 1.08 e⁻) within the created C—C bond.

It is also noticed from Tables 2 and 3 that the total weight of palladium in the palladium-ligand bonds increases of about 0.25 electrons during the reductive elimination, for example in the case triphenylphosphine ligand and with 2 phenyl groups attached to the metal, the weight of the back-donation into the ligands varies from 0.21 to 0.35 by bond. Similarly, with carbene as a ligand and 2 methyl groups as substituents, the weight of the back-donation varies from 0.16 to 0.27 by bond. Therefore, what is formally a metal reduction appears to be a transfer of electrons from the substituents toward the ligands.

Confirmations through an ELF monitored intrinsic reaction coordinate (IRC) computations

To illustrate our findings, we propose to provide a detailed ELF analysis of a full reaction path computed using an IRC

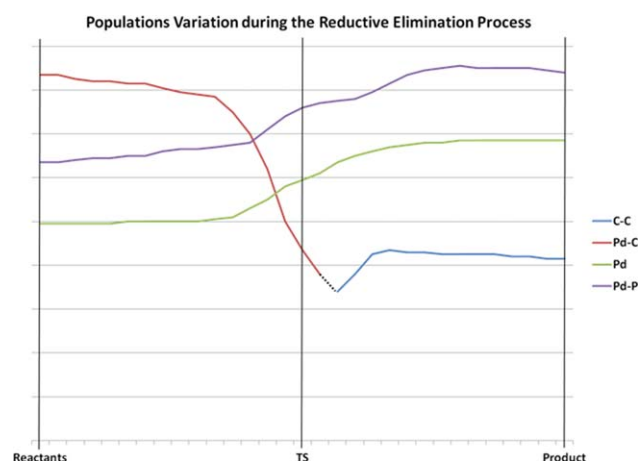
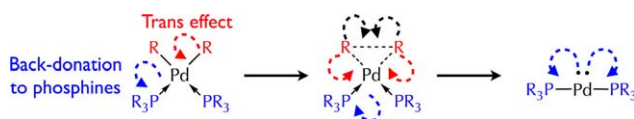


Figure 3. ELF analysis of the populations for various bonds during a full reaction path for system A/Ph3 with methyl-methyl. Scales for Pd and Pd-P have been adjusted to visualise the transfers. Actual numerical values are provided in Supporting Information.



Scheme 3. Proposed mechanism for reductive elimination. [Color figure can be viewed in the online issue, which is available at wileyonlinelibrary.com.]

computation (15 study points have been added between each reaction steps). Figure 3 displays the variation of the populations during the reductive elimination process within the palladium complex. For sake of simplicity we chose to present the smallest complex: system A/PH₃ with methyl–methyl. As we can see, the two Pd–C bonds (see red curve) vanish while the C–C bond (see blue curve) is created. Meanwhile, the blue curve does not reach the same level of population as the two Pd–C bonds ones (red curve). Overall, this is compensated by both the enrichment of the two Pd–P bonds (violet curve) due to the earlier described trans-effect, and to the reduction of the palladium (green curve). This is the proof that an electron transfer occurs as described previously and provides a visualization of the phenomenon.

Conclusions

The proposed computational strategy based on quantum topological analyses allows a deeper understanding of the interactions between the constitutive elements of a reactive organometallic complex. The coupled QTAIM/ELF partitioning used here is able to dissect the electronic rearrangement along a chemical pathway. This methodology was applied here to reinvestigate a classical process in organometallic chemistry, namely the reductive elimination and more specifically the one induced by palladium. The first result arises from the coordination mode of the ligands (i.e., phosphine, carbene) commonly described in first approximation as dative. It appears that the lone pair stays centered on the ligand: the associated electronic domain, as obtained from the ELF analysis, being effectively shared between the metal and the ligand but with a strong electron delocalization toward the phosphine and the carbene. The second important result emerges from the QTAIM/ELF dual partitioning approach that allows separating the respective contributions to the ELF bonding domain into atomic contributions. Through a strong trans effect coming from the carbon involved in the reductive elimination, the palladium center delocalizes valence electrons toward the phosphine (see Scheme 3). This has been discussed experimentally but is for the first time formalized, using a combined topological approach. Moreover, an important new point is that the same tendency is found for carbene-based system. Thus, the back-donation is a key component of the stabilization of the complexes. As the computational data obtained here indicate its increase during the reductive elimination, one of the key components of the reaction is the ability of the palladium ligands to accept back-donated electrons. This explains the observed trends regarding reductive elimination in organometallic chemistry and overall this contribution proposes a ration-


alization of such a fine electronic structure phenomena by using a new topological approach. A clear visualization of the phenomenon has been provided using the complete ELF monitoring of the atoms' populations during a reaction path (through IRC). From a methodological point of view, the present strategy enables a straightforward way to separate donation from back donation in the spirit of the DCD model but providing a more detailed picture (i.e., including more effects through the topology partition such as subvalence). We expect that other elementary (organometallic) reactions can be reinvestigated by the QTAIM/ELF methodology and will give clues about the real electrons delocalization fluxes that could help the experimental organometallic community to improve the design of palladium-catalysed systems. For a limited computational cost thanks to the capabilities of the TOPMOD 09 code, one can have access to a tool, which has proven here to be suitable to dissect the contributions of each partner involved in bonding within a complex system. This method grounded solely on the electronic density extracted from a wave function is generalizable to any reactions of interest.

Acknowledgments

The authors thank Pr. Giovanni Poli and Serge Thorimbert for careful reading of the manuscript, the Emergence program of UPMC is acknowledged for funding the post-doctoral position of B. de C.

Keywords: topological analysis · organometallics

How to cite this article: B. de Courcy, E. Derat, J.-P. Piquemal. *J. Comput. Chem.* **2015**, *36*, 1167–1175. DOI: 10.1002/jcc.23911

 Additional Supporting Information may be found in the online version of this article.

- [1] C. C. C. Johansson Seechurn, M. O. Kitching, T. J. Colacot, V. Snieckus, *Angew. Chem. Int. Ed.* **2012**, *51*, 5062.
- [2] T. W. Lyons, M. S. Sanford, *Chem. Rev.* **2010**, *110*, 1147.
- [3] J. K. Stille, *Angew. Chem. Int. Ed.* **1986**, *25*, 508.
- [4] C. E. I. Knappke, J. von Wangelin, *Chem. Soc. Rev.* **2011**, *40*, 4948.
- [5] Q. Liu, Y. Lan, J. Liu, G. Li, Y.-D. Wu, A. Lei, *J. Am. Chem. Soc.* **2009**, *131*, 10201.
- [6] A. Suzuki, *Angew. Chem. Int. Ed.* **2011**, *50*, 6722.
- [7] T. Hiyama, Y. Nakao, *Chem. Soc. Rev.* **2011**, *40*, 4893.
- [8] (a) G. Maestri, E. Motti, N. Della Ca, M. Malacria, E. Derat, M. Catellani, *J. Am. Chem. Soc.* **2011**, *133*, 8574; (b) E. Derat, G. Maestri, *WIREs Comput. Mol. Sci.* **2013**, *3*, 529.
- [9] L. Xue, Z. Lin, *Chem. Soc. Rev.* **2010**, *39*, 1692.
- [10] (a) J. J. Low, W. A. Goddard, *J. Am. Chem. Soc.* **1986**, *108*, 6115; (b) J. J. Low, W. A. Goddard, *Organometallics* **1986**, *5*, 609.
- [11] (a) M. Pérez-Rodríguez, A. A. C. Braga, M. García-Melchor, M. H. Pérez-Temprano, J. A. Casares, G. Ujaque, A. R. de Lera, R. Álvarez, F. Maseras, P. Espinet, *J. Am. Chem. Soc.* **2009**, *131*, 3650; (b) M. Pérez-Rodríguez, A. A. C. Braga, A. R. de Lera, F. Maseras, R. Álvarez, P. Espinet, *Organometallics* **2010**, *29*, 4983; (c) M. García-Melchor, A. A. C. Braga, A. Lledós, G. Ujaque, F. Maseras, *Acc. Chem. Res.* **2013**, *46*, 2626; (d) V. P. Ananikov, D. G. Musaev, K. Morokuma, *Eur. J. Inorg. Chem.* **2007**, 2007, 5390.
- [12] (a) D. C. Powers, T. Ritter, *Nat. Chem.* **2009**, *1*, 302; (b) D. C. Powers, D. D. Benitez, E. Tkatchouk, W. A. Goddard, T. Ritter, *J. Am. Chem. Soc.* **2010**, *132*, 14092.

- [13] W. Shi, Y. Luo, X. Luo, L. Chao, H. Zhang, J. Wang, A. Lei, *J. Am. Chem. Soc.* **2008**, *130*, 14713.
- [14] M. Alcarazo, T. Stork, A. Anoop, W. Thiel, A. Fürstner, *Angew. Chem. Int. Ed.* **2010**, *49*, 2542.
- [15] J. F. Hartwig, *Inorg. Chem.* **2007**, *46*, 1936.
- [16] M. Yamashita, J. V. Cuevas Vicario, J. F. Hartwig, *J. Am. Chem. Soc.* **2003**, *125*, 16347.
- [17] (a) M. J. S. Dewar, *Bull. Soc. Chim. Fr.* **1951**, *18*, C71; (b) J. Chatt, L. A. Duncanson, *J. Chem. Soc.* **1953**, 2939–2947. DOI:10.1039/JR9530002939.
- [18] (a) G. Frenking, N. Frohlich, *Chem. Rev.* **2000**, *100*, 717; (b) A. Dedieu, *Chem. Rev.* **2000**, *100*, 543; (c) G. Frenking, *J. Organomet. Chem.* **2001**, *635*, 9.
- [19] P. S. Bagus, K. Hermann, C. W. Bauschlicher, *J. Chem. Phys.* **1984**, *80*, 4378.
- [20] T. Ziegler, A. Rauk, *Theor. Chim. Acta.* **1977**, *46*, 1.
- [21] G. Pacchioni, P. S. Bagus, *Inorg. Chem.* **1992**, *31*, 4391.
- [22] M. Linares, B. Braida, S. Humbel, *Inorg. Chem.* **2007**, *46*, 11390.
- [23] (a) A. D. Becke, K. E. Edgecombe, *J. Chem. Phys.* **1990**, *92*, 5397; (b) B. Silvi, A. Savin, *Nature*, **1994**, *371*, 683.
- [24] (a) G. Jansen, M. Schubart, B. Findeis, L. H. Gade, I. J. Scowen, M. McPartlin, *J. Am. Chem. Soc.* **1998**, *120*, 7239; (b) G. Jansen, In *Chemical Bonding: State of the Art in Conceptual Quantum Chemistry* J. G. Angyan, B. Silvi, Eds.; La Colle-sur-Loup, France, **2000**, p. 42; (c) S. Raub, G. Jansen, *Theor. Chem. Acc.* **2001**, *106*, 223; (d) N. Gillet, R. Chaudret, J. C. Garcia, W. Yang, B. Silvi, J.-P. Piquemal, *J. Chem. Theory Comput.* **2012**, *8*, 3993; (e) G. Aullón, S. Alvarez, *Theor. Chem. Acc.* **2009**, *123*, 67; (f) J. Pilmé, B. Silvi, M. Alikhani, *J. Phys. Chem. A* **2003**, *107*, 4506; (g) B. Silvi, J. Pilmé, F. Fuster, E. M. Alikhani, In *Metal-Ligand Interactions in Molecular, Nano, Micro, and Macro-Systems in Complex Environments*, NATO-ASI series, N. Russo, M. Witko, Eds.; Kluwer: Dordrecht, **2003**; pp. 241.
- [25] (a) R. W. Bader, *Atoms in Molecules: A Quantum Theory*; Oxford University Press: Oxford, **1990**; (b) P. L. A. Popelier, *Atoms in Molecules: An Introduction*; Prentice-Hall: Harlow, **2000**. (c) R. F. W. Bader, *Atoms in Molecules: A Quantum Theory*; Oxford University Press: Oxford, **1990**. (d) R. F. W. Bader, *Chem. Rev.* **1991**, *91*, 893; (e) P. L. A. Popelier, In *Structure and Bonding: Intermolecular Forces and Clusters I*; D. J. Wales, Ed.; Springer: Heidelberg, **2005**; p. 1; (f) P. L. A. Popelier, P. J. Smith, In *Specialist Periodical Reports Chemical Modelling: Applications and Theory*; A. Hinchliffe, Ed.; The Royal Society of Chemistry: Cambridge, **2002**; p. 391.; (g) P. L. A. Popelier, F. M. Aicken, S. E. O'Brien, In *Specialist Periodical Reports Chemical Modelling: Applications and Theory*; A. Hinchliffe, Ed.; The Royal Society of Chemistry: Cambridge, **2000**; p. 143.
- [26] P. K. Sajith, C. H. Suresh, *Inorg. Chem.* **2011**, *50*, 8085.
- [27] (a) P. González-Navarrete, L. R. Domingo, J. Andrés, S. Berski, B. Silvi, *J. Comput. Chem.* **2012**, *33*, 2400; (b) J. Andrés, P. González-Navarrete, V. S. Safont, *Int. J. Quantum Chem.* **2014**, *114*, 1239; (c) J. Andrés, L. Gracia, P. González-Navarrete, V.S. Safont, *Comput. Theor. Chem.* **2015**, *1053*, 17; (d) D. Fang, R. Chaudret, J.-P. Piquemal, G. A. Cisneros, *J. Chem. Theory Comput.* **2013**, *9*, 2156.
- [28] J.-P. Piquemal, A. Marquez, O. Parisel, C. Giessner-Prettre, *J. Comput. Chem.* **2005**, *26*, 1052.
- [29] F. Weigend, R. Ahlrichs, *Phys. Chem. Chem. Phys.* **2005**, *7*, 3297.
- [30] K. A. Peterson, D. Figgen, M. Dolg, H. Stoll, *J. Chem. Phys.* **2007**, *126*, 124101.
- [31] M. J. Frisch, G. W. Trucks, H. B. Schlegel, G. E. Scuseria, M. A. Robb, J. R. Cheeseman, G. Scalmani, V. Barone, B. Mennucci, G. A. Petersson, H. Nakatsuji, M. Caricato, X. Li, H. P. Hratchian, A. F. Izmaylov, J. Bloino, G. Zheng, J. L. Sonnenberg, M. Hada, M. Ehara, K. Toyota, R. Fukuda, J. Hasegawa, M. Ishida, T. Nakajima, Y. Honda, O. Kitao, H. Nakai, T. Vreven, J. A. Montgomery, Jr., J. E. Peralta, F. Ogliaro, M. Bearpark, J. J. Heyd, E. Brothers, K. N. Kudin, V. N. Staroverov, R. Kobayashi, J. Normand, K. Raghavachari, A. Rendell, J. C. Burant, S. S. Iyengar, J. Tomasi, M. Cossi, N. Rega, J. M. Millam, M. Klene, J. E. Knox, J. B. Cross, V. Bakken, C. Adamo, J. Jaramillo, R. Gomperts, R. E. Stratmann, O. Yazyev, A. J. Austin, R. Cammi, C. Pomelli, J. W. Ochterski, R. L. Martin, K. Morokuma, V. G. Zakrzewski, G. A. Voth, P. Salvador, J. J. Dannenberg, S. Dapprich, A. D. Daniels, Ö. Farkas, J. B. Foresman, J. V. Ortiz, J. Cioslowski, and D. J. Fox, Gaussian 09, Revision A02; Gaussian, Inc.: Wallingford, CT, **2009**.
- [32] M. Dupuis, A. Marquez, E. R. Davidson, HONDO95.3, Quantum Chemistry Program Exchange (QCPE); Indiana University: Bloomington, IN.
- [33] S. Noury, X. Krokidis, F. Fuster, B. Silvi, *J. Comput. Chem.* **1999**, *23*, 597.
- [34] B. de Courcy, L. G. Pedersen, O. Parisel, N. Gresh, B. Silvi, J. Pilmé, J.-P. Piquemal, *J. Chem. Theory Comput.* **2010**, *6*, 1048.
- [35] C. Liu, H. Zhang, W. Shi, A. Lei, *Chem. Rev.* **2011**, *111*, 1780.
- [36] (a) Z. Lin, M. B. Hall, *Inorg. Chem.* **1991**, *30*, 646; (b) B. Pinter, V. Van Speybroeck, M. Waroquier, P. Geerlings, F. De Proft, *Phys. Chem. Chem. Phys.* **2013**, *15*, 17354.
- [37] A. Marjolin, C. Gourlaouen, C. Clavaguera, J.-P. Dognon, J.-P. Piquemal, *Chem. Phys. Lett.* **2013**, *563*, 25.
- [38] Y. Zhao, D. G. Truhlar, *J. Phys. Chem. A* **2006**, *110*, 13126.

Received: 27 October 2014
Revised: 14 February 2015
Accepted: 9 March 2015
Published online on 21 April 2015